



# Lawrence Berkeley Laboratory

UNIVERSITY OF CALIFORNIA

## Materials & Molecular Research Division

Submitted to Surface Science

LEED INTENSITY ANALYSIS OF THE (1 x 5)  
RECONSTRUCTION OF Ir(100)

E. Lang, K. Müller, K. Heinz, M.A. Van Hove,  
R.J. Koestner, and G.A. Somorjai

July 1982

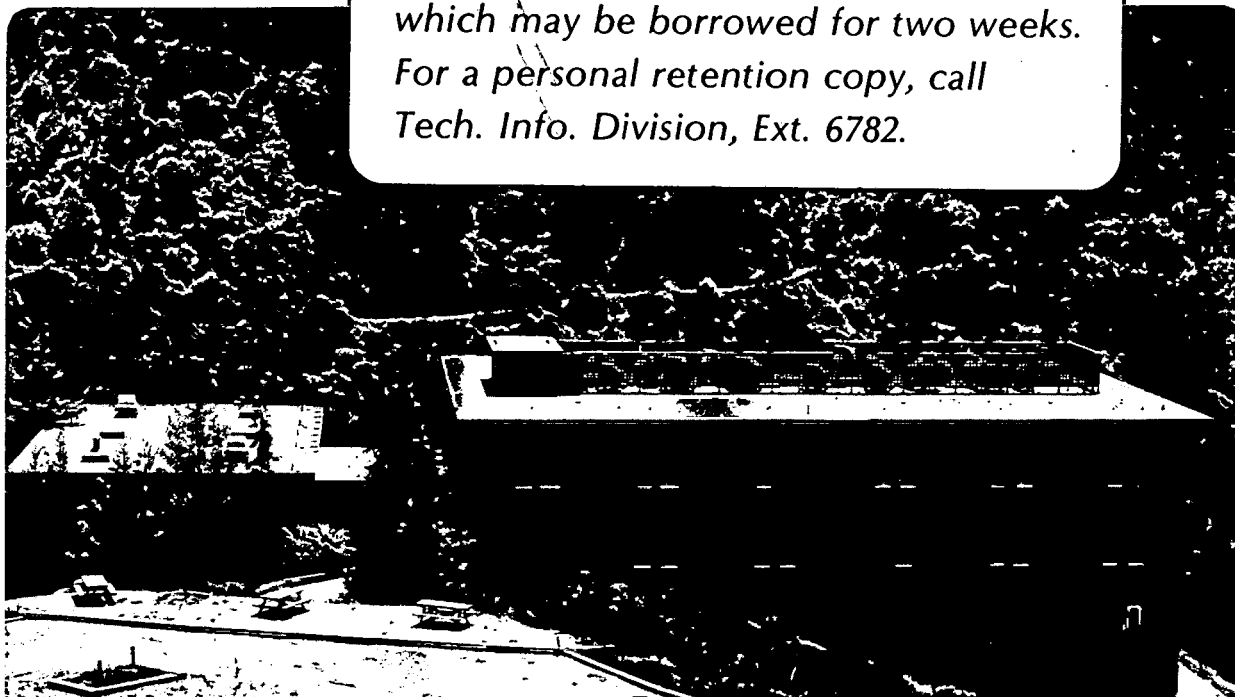
RECEIVED  
LAWRENCE  
BERKELEY LABORATORY

JUL 16 1982

LIBRARY AND  
DOCUMENTS SECTION

### TWO-WEEK LOAN COPY

*This is a Library Circulating Copy  
which may be borrowed for two weeks.  
For a personal retention copy, call  
Tech. Info. Division, Ext. 6782.*



## **DISCLAIMER**

This document was prepared as an account of work sponsored by the United States Government. While this document is believed to contain correct information, neither the United States Government nor any agency thereof, nor the Regents of the University of California, nor any of their employees, makes any warranty, express or implied, or assumes any legal responsibility for the accuracy, completeness, or usefulness of any information, apparatus, product, or process disclosed, or represents that its use would not infringe privately owned rights. Reference herein to any specific commercial product, process, or service by its trade name, trademark, manufacturer, or otherwise, does not necessarily constitute or imply its endorsement, recommendation, or favoring by the United States Government or any agency thereof, or the Regents of the University of California. The views and opinions of authors expressed herein do not necessarily state or reflect those of the United States Government or any agency thereof or the Regents of the University of California.

LEED INTENSITY ANALYSIS OF THE (1 x 5) RECONSTRUCTION OF Ir(100)

E. Lang, K. Müller and K. Heinz

Institut für Angewandte Physik, Lehrstuhl für Festkörperphysik  
der Universität Erlangen-Nürnberg, Erwin-Rommel-Straße 1,  
D-8520 Erlangen, GERMANY

and

M.A. Van Hove, R.J. Koestner and G.A. Somorjai

Materials and Molecular Research Division,  
Lawrence Berkeley Laboratory and  
Department of Chemistry,  
University of California, Berkeley  
Berkeley, California 94720, USA

## 1. INTRODUCTION

The crystallography of relatively complicated ordered surface structures is a challenging task for any surface-sensitive technique. In such structures many non-equivalent atoms exist, all of whose independent coordinates must be found. Among the more complex structures studied to date is the (1 x 5) reconstruction of the clean Ir(100) surface. This surface involves six atoms per surface unit cell in the topmost layer, at least for the most popular structural model, which consists of a quasi-hexagonally topmost atomic layer that is nearly hexagonally close-packed and rests on the square-lattice substrate layer with a (1 x 5) coincidence unit cell.<sup>(1,2)</sup> If one allows this quasi-hexagonal layer to buckle and otherwise distort under the influence of the substrate, and if one ignores any distortions in the substrate itself, there are  $6 \times 3 = 18$  coordinates to be determined. For quasi-hexagonal models that additionally maintain two mutually orthogonal mirror planes perpendicular to the surface, the quasihexagonal model still involves six independent atomic coordinates.

In circumstances where many structural parameters are available, there is a particular danger of ending up with a local minimum rather than the global minimum in the disagreement between theory and experiment (i.e., one may find a structure that is best with respect to small changes in all coordinates, but that may be worse than some other very different structure). It is therefore very useful to include in such structural determinations not only a large amount of data and a large number of trial structures, but also reliability checks. Important among such checks are independent measurements which reinforce the experimental reproducibility and quantitative reliability factors which enhance the objectivity of the structural search.

In a previous Low Energy Electron Diffraction (LEED) study,<sup>(1,2)</sup> the structure of Ir(100)(1 x 5) was investigated in some detail with the help of an extensive set of intensity vs. energy (I-V) spectra, taken at several incidence angles. A set of corresponding LEED calculations covering over 100 structures belonging to several different classes of surface models was performed. A limitation in that work was the inability to apply reliability factors (R-factors) as a result of gaps in the experimental I-V curves where the intensities fell below the film threshold of the photographic data acquisition method.

The recent new measurement in Erlangen of I-V spectra for the Ir(100)(1 x 5) surface gives a two-fold opportunity to check the previous work and enhance the reliability of its structural results: 1) an independent set of data is now available that was obtained in a different laboratory by a very different method, using a Vidicon camera and different data manipulation (especially for background subtraction, which is a matter of some concern with the closely-spaced diffraction spots for this surface structure, and precise definition of normal incidence including symmetrical beam averaging); 2) the new data have no gaps and, therefore, allow the use of R-factors. On the other hand, the new data set, unlike the previous one, does not include measurements away from normal incidence; however, the total energy range of actual measurements that overlap with the theoretical curves is comparable in the two sets of experiments.

No changes have been introduced in the LEED theory or in the parameters used in the calculations performed earlier, so that we could simply reuse the calculated I-V curves already reported in the previous study.

The result of the present structural determination of Ir(100)(1 x 5) will be shown to confirm that of the previous study<sup>(1,2)</sup> within 0.2Å for the atomic positions. In addition, the second structural choice of the previous work, a model consisting of shifted close-packed rows of surface atoms, is now more

clearly ruled out.

## 2. EXPERIMENTAL PROCEDURE

The LEED intensities for Ir(100)(1 x 5) were measured in an UHV chamber with a working pressure in the  $10^{-10}$  mbar range using a 4 grid LEED optics (P 20 Phosphor, 8kV screen voltage). The crystal (MRC) was oriented to within  $\pm 1^\circ$  of the (100) plane. It was cleaned by argon ion bombardment and several cycles of heating in  $O_2$  ( $10^{-8}$  to  $10^{-7}$  mbar, 1400 K) and in UHV (1800 K), until it yielded a sharply focused low-background (1 x 5) pattern and no impurities (C, Ca) were detectable by Auger Electron Spectroscopy (AES).

The intensities of the Ir(100)(1 x 5) diffraction spots were taken at  $T \approx 100$  K. A computer controlled television camera was used to perform high speed measurements, typically of the order of minutes per spectrum. The method, which allows to take spectra of a number of spots within a reasonable period of time including proper background subtraction, has been described earlier in detail.<sup>(3-6)</sup> Therefore, it will only briefly be outlined in the following.

A video camera receives the optical intensity signal from the luminescent LEED screen and transfers the corresponding electronic signal via a digitizing interface to a processing computer. An electronic window generated by the computer and made visible on the monitor allows the selection of a single diffraction spot. The electronic signal is integrated within the window and the background level determined at its edge is subtracted. The resulting integral intensity is put into the computer memory and the respective primary beam current is stored as well for final normalization. In order to be properly correlated with the intensity data, the electron energy is checked each time before it is stepped up 1 eV or less by a computer controlled voltage supply. The electronic

window is readjusted in order to center the spot at its new position and the whole procedure of measurement is repeated. In this way the intensity-energy spectrum develops automatically under software control. It is also possible to switch the electronic window to several preselected spots at each energy before stepping up the energy. As described in Reference 6, several modes of integration exist whose measuring time consumptions vary from about 0.4 sec down to 0.02 sec per intensity-energy point. So, for example, a spectrum of 300 points is taken within two minutes in the low speed mode and within 6 sec in the high speed mode.

When the LEED pattern contains a large number of spots, as in the case of reconstructed Ir(100), the spatial resolution of the intensity measurement becomes important. The relevant properties of the TV system are demonstrated in Figure 1. In the upper panel the Ir(100)(1 x 5) pattern at an energy of  $E = 365$  eV is shown as displayed on the monitor. The horizontal white line is a degenerate form of the electronic window chosen in order to perform a cut through an array of diffraction spots. The result of the intensity distribution along this line is shown in the middle panel of Figure 1. For that particular energy the  $(2/5, \bar{1})$  and  $(4/5, \bar{1})$  spots appear to be very weak so that they scarcely show up in the profile. The spatial resolution in the vertical direction is given by the distance of horizontal TV lines, which is 1/300 of the TV frame. For the camera-screen distance used, this corresponds to a resolution of the diffraction angle of about  $0.3^\circ$ . The horizontal spatial resolution depends on the rate of digitization of the electronic signal and again a value of  $0.3^\circ$  results for the parameters used. In the lowest panel of Figure 1 the intensity profile is displayed on an expanded scale. This frame shows that crowded superstructure spots are well resolved even at the comparatively high energy of 365 eV as it is particularly demonstrated for the  $(1/5, \bar{1})$  and  $(0\bar{1})$

spots.

However, crowding of spots demands increased care in the procedure of background determination. It particularly excludes the use of the region between two spots for defining the background level. In the present case of Ir(100) the intensity level of a spot decreases only to 1/5 of its maximum value at the position of the neighbor spot when Lorentz-shaped profiles are assumed.<sup>(7)</sup> Therefore, the determination of the background level between closely spaced spots implies the risk that their respective intensity spectra are to some extent mixed. This can only be avoided by selecting an area for background determination which is only negligibly influenced by neighbor spots. For Ir(100)(1 x 5) this implies measuring the background level along a line towards the dark center of the unit mesh rather than along the side of a unit mesh. The influence of erroneous background subtraction has been demonstrated in an investigation<sup>(7)</sup> dealing with the reconstructed (100) surface of Pt which shows a diffraction pattern similar to that of reconstructed Ir(100) (basically, all Ir spots are split into multiplets in the case of Pt). Figure 2 gives the results obtained from the (1, 2/5) spot doublet. The spectra are labeled "correct" and "false" corresponding to a correct or incorrect background determination as described above. The difference spectrum between the correct and false spectra shows considerable structure. In the bottom part of Figure 2 the sum of the (1, 1/5) and (1, 3/5) doublet spectra is given which are direct neighbors of the (1, 2/5) spot. It turns out that the main features of the (1, 1/5) difference spectrum are clearly related to intensity peaks of neighbor beams. Incorrect background determination therefore leads to a mixing of intensities of different spots. Care was taken to avoid this error in the measurements of Ir(100) beam intensities to be presented below.

Usually another source of error arises as a result of some uncertainty in

the value of the angle of incidence. Considerable modifications of the spectra can be observed when the angle of incidence is changed by only half a degree. This is also true near normal incidence, which is in many cases used to reduce the size of dynamical LEED calculations by symmetry arguments. The sensitivity to misalignment is demonstrated in Figure 3 where spectra of the  $(1, 1/5)$  beam of Ir(100)(1 x 5) are displayed for different misalignments. The first pair of spectra compares the results of two measurements for which the deviations from ideal normal incidence were not larger than  $0.5^\circ$ . Considerable differences in the spectra appear in the low energy regime and in the region near 200 eV. Even for a more precise adjustment of normal incidence, i.e. for  $\theta < 0.2^\circ$ , less pronounced but still detectable modifications are observed as demonstrated in the lower part of Figure 3. Fortunately, however, the normal incidence condition allows one to reduce the influence of residual misalignment by a simple averaging procedure. As already described earlier,<sup>(6,8,9)</sup> all symmetrically equivalent beams are measured and finally averaged. The resulting mean spectrum shows only negligible differences with respect to that for ideal normal incidence. It has been demonstrated for the Ni(100) surface that even for misalignments of up to  $\theta \approx 3^\circ$  the averaged spectrum is undisturbed.<sup>(6)</sup> This means that the deviations of the intensities of equivalent beams vary linearly with small misalignment. Deviations therefore cancel by averaging and the ideal spectrum results with sufficiently good approximation. Figure 4 demonstrates the averaging for the  $(10)$  beam of Ir(100)(1 x 5). The primary beam was set to normal incidence by comparing the spectra of the equivalent beams  $(01)$ ,  $(\bar{1}0)$ ,  $(0\bar{1})$  and  $(10)$ , which are shown for the best adjustment achieved. Only minor discrepancies appear, possibly caused by defects in the luminescent screen. So it can be assumed that the averaged spectrum approximates the correct one to a high degree. This is a strong argument for taking measurements at normal inci-

dence of the primary beam.

Recently it has been reported that LEED data taken by high speed methods can be erroneous.<sup>(10)</sup> It was pointed out that the measurement speed is limited by the time needed for the redistribution of electric fields between the grids, in order to avoid non-linear energy scaling. Moreover, the importance of magnetic field compensation was stressed and proposed to be performed at each single energy or energy interval. Therefore, the influence of speed was checked with the equipment used for the present measurements. Figure 5 gives the results for the (11) beam of Ir(100) measured at speeds from 25 eV/s down to 0.2 eV/s using a corresponding number of TV half-frames for each point of measurement. It appears that only negligible differences result. Concerning the influence of stray magnetic fields it is clear that a high speed measurement should do without energy dependent field compensation. In the present measurement Helmholtz coils were used to reduce the magnetic field at the sample. The criterion for best constant compensation was the agreement of the spectra of symmetrically equivalent beams as demonstrated in Figure 4. Moreover, it should be pointed out that a residual influence of magnetic fields can be expected to be canceled to a high degree by averaging, since in this case the intensities are only affected by the direction of the incident primary beam. However, we feel that more careful investigations on the subject of stray electromagnetic fields should be done in order to settle the problem.

In Figure 6 and Figure 7 the results taken at  $T \approx 100$  K are given for an energy range up to 500 eV, although only the low energy part is used for comparison with the calculations. The data were taken with a rate of 0.4 energy points/second whereby a step width of  $\Delta E = 0.5$  eV was used. Twelve symmetrically independent beams are presented all of which have been averaged with their symmetrically equivalent counterparts. Compared with the results of the earlier

work<sup>(1,2)</sup> no breaks in the energy range occur. As expected, the intensities are confirmed to be very low within the breaks of the former data, such as in the case of the (0, 3/5) spot for energies between 60 eV and 200 eV. The structure of the spectra is more pronounced than in References 1 and 2 which is certainly due to the different treatment of background subtraction.

In Figure 8, we compare the normal-incidence data taken at Erlangen with those taken at Berkeley in the energy range up to about 120 eV, the highest energy used in the calculations (since the new data are referred to the Fermi level, which is about 6 eV below the vacuum level used as a reference in the Berkeley data, the latter data have been shifted accordingly).

Some differences in relative peak heights between the two sets of data are due to the difference in temperature ( $\sim 100$  K vs.  $\sim 310$  K), which is in principle significant in view of the relatively small Debye temperature of iridium ( $\sim 392$  K). In particular, the lower temperature of the Erlangen data explains the relatively larger intensities found at the higher energies. However, temperature differences rarely affect peak positions in I-V curves, on which the structural determination depends primarily. Some discrepancies observed between the two data sets are of a more serious nature, since they involve shifts in peak positions. We can only speculate on the possible causes of these discrepancies. Apart from the obvious causes, such as misalignment of the incident beam and different data-acquisition methods, we can suggest the possibility that impurities or the different temperatures can affect the two surface structures differently and that the diffraction is quite sensitive to minor relative displacements in the complicated reconstructed layers (such sensitivity has been observed in our calculations). Indeed, the final structural predictions based on the two sets of data will be seen to differ slightly, although within the uncertainty limits of the method.

### 3. LEED THEORY

The theoretical methods and parameters are described in Reference 2. Briefly, the Combined Space Method<sup>(11)</sup> was applied, in which the multiple scattering within the reconstructed layer and within each substrate layer is treated in the spherical-wave expansion and the multiple scattering between layers is treated in the plane-wave representation. The convergent Reverse Scattering Perturbation method is used within the reconstructed layer, which contains five or six atoms per unit cell, depending on the class of structure examined. Two iridium scattering potentials of the muffin-tin form were used: the first was a non-relativistic band structure potential by Arbman and Hoernfelt,<sup>(12)</sup> the second a modification of the first one by Feder<sup>(13)</sup> to include relativistic effects. Six phase shifts were used ( $l_{\max} = 5$ ). The muffin-tin zero level chosen in the calculation was 15 eV below the vacuum level, which is later varied by a rigid energy shift in the comparison with experiment. It should be added that our calculations were performed at 300 K for comparison with the earlier data, whereas the new data were measured at  $\sim 100$  K: as was mentioned in the last Section, it is known that structural determination depends only marginally on the temperature used in the calculations and we therefore ignore this effect.

From the 139 geometrical models examined for Ir(100)(1 x 5) in Reference 2, we selected 56 of the more promising ones for the present comparison with the new data. Most of these are based on a quasi-hexagonal top layer, with different registries with respect to the substrate and different amounts of buckling, cf. Figure 9. To this class belongs the structure favored in our previous study. Another set of structures is based on shifting selected rows of atoms into closer-packed arrangements, cf. Figures 11c, d and e of Reference

1, without increasing the average coverage (such an increase does take place with the hexagonal models). The previous study could not exclude some of these structures, as they gave almost as good agreement with experiment as the preferred one. Finally, some models based on a charge-density-wave (CDW) reconstruction are also considered here as representatives of a radically different kind of surface structure: here a CDW with a wavelength of 5 lattice constants with atomic displacements perpendicular to the surface is considered. In all models that we investigated the substrate below the simple reconstructed layer is kept bulk-like.

As the new experimental data present no gaps in the available energy range, it is appropriate to apply R-factors to evaluate the level of agreement between theory and experiment for the various structural models. We use the following R-factors together with their average:

ROS = fraction of energy range with slopes of opposite signs in the experimental and theoretical I-V curves,

$$R1 = 0.75 \int |I_e - cI_t| dE / \int |I_e| dE,$$

$$R2 = 0.5 \int (I_e - cI_t)^2 dE / \int I_e^2 dE,$$

$$RRZJ = 0.5 \int \{ |I_e'' - cI_t''| |I_e' - cI_t'| / (|I_e'| + \max |I_e'|) \} dE / (0.027 \int |I_e| dE),$$

$$RPE = 0.5 \int (Y_e - Y_t)^2 dE / \int (Y_e^2 + Y_t^2) dE, Y(E) = L / (1 + V_{oi}^2 L^2), L = I'/I$$

Here  $c = \int |I_e| dE / \int |I_t| dE$  and the apostrophe denotes differentiation with respect to the energy. RRZJ is the reduced Zanazzi-Jona R-factor,<sup>(14)</sup> while RPE is Pendry's R-factor,<sup>(15)</sup> both renormalized with a factor 0.5 to match the scale of the other R-factors ( $V_{oi}$  is an estimate of the imaginary part of the inner potential, here 4 eV). We shall mainly use the average over these five R-factors, but we shall also quote 2 x RRZJ and 2 x RPE to allow comparison with other work.

#### 4. RESULTS AND DISCUSSION

##### Surface Structure

In Table I we summarize the comparison between theory and experiment for different groups of structures, indicating the best spacing between top layer and substrate for each group and corresponding R-factors. It is clear that the bridge-registered quasi-hexagonal top layer is the preferred structure and that the buckling of this top layer is close to its "maximum" amount. This maximum buckling is defined as the buckling obtained by assuming bulk interatomic distances between all bonding partners in all layers, as illustrated in Figure 9: the maximum distance between nuclear planes of the layer with bridge registry for full buckling is then  $0.48\text{\AA}$ . With "2/3 buckling" this layer thickness is reduced to  $2/3 \times 0.48 = 0.32\text{\AA}$ .

The spacing between the top layer and the substrate is best determined by considering the plot of the average R-factor as a function of that spacing, cf. Figure 10: it appears to lie around  $2.02 \pm 0.05\text{\AA}$ . This represents a fairly large contraction by  $0.2\text{\AA}$  compared with the layer spacing that one would predict on the basis of bulk bond lengths. The best spacing found for the corresponding 2/3-buckled layer is almost  $0.1\text{\AA}$  larger than for the full-buckled layer: this can be understood from the fact that this layer is about  $0.48/3 = 0.16\text{\AA}$  thinner, so that an expansion of the spacing by about  $0.16/2 \sim 0.1\text{\AA}$  is required to keep constant the height of the central plane of gravity of the layer over the substrate (we define the layer spacing to be the distance between the substrate and that nuclear plane of the reconstructed layer which is closest to the substrate). The central plane of gravity of a layer appears to play a special role, as has already been noticed in past LEED calculations<sup>(16)</sup>: atomic movements that leave unchanged the central plane of gravity of a layer have less effect on I-V curves than those that do move the central plane of

gravity (in general the word "gravity" should probably be replaced by "scattering strength" when different chemical elements are present). Figure 11 shows representative I-V curve comparisons for various layer spacings with bridge-registered quasi-hexagonal models.

Table I discriminates clearly against the shifted-rows models, one of which was found to be almost equally acceptable as the best quasi-hexagonal model in the previous study (on the basis of only normal-incidence data, as is also the case here).

#### Scattering Potential

Table I and Figures 10 and 11 also exhibit the effect of a relativistic correction to the iridium scattering potential. In this instance, no noteworthy gain in the agreement with experiment is obtained with this correction, as was already concluded in the previous work, although individual I-V curves can be strongly affected by the change in potential. Furthermore, the structural result is not significantly affected. The reason for considering this relativistic correction lies in the generally unsatisfactory agreement between LEED theory and experiment for surfaces of the 5d metals (specifically W, Ir, Pt and Au): one possible cause is a relativistic effect.

Although Feder obtains a better fit with experimental spin-polarization data in LEED by inclusion of a relativistic correction to the potential, this modification apparently is not so effective for the LEED intensities themselves, according to Feder's work on Pt(111)<sup>(17)</sup> as well as separate work on Pt(111)<sup>(18)</sup> using the same potential and correction, and the Ir(100)(1 x 5) work discussed here. It remains, therefore, unclear what the cause of the general difficulty with the 5d metals is.

## 5. CONCLUSIONS

In summary, new experimental LEED data for the reconstructed Ir(100)(1 x 5) surface have been taken with a video camera coupled to a computer for the generation of I-V curves. Special attention was paid to minimize the effect of uncertainties in the angle of incidence (including those due to residual magnetic fields) and to assure proper background subtraction.

These data have been compared with existing calculated LEED I-V curves to determine the surface structure. An R-factor comparison was made, which was not possible in a previous study using incomplete data. The basic structural conclusion of the previous study has been confirmed, yielding a quasi-hexagonal reconstructed top layer involving bridge sites with respect to the underlying substrate layer. The top layer may be more buckled than previously thought, but the differences in atomic positions are of the order of the uncertainty of the determination (0.1Å). A slightly larger contraction of the top layer spacing is found here, which would translate to about 5% bond length contractions between atoms in the top layer and in the next layer. The best structure yields a five-R-factor average of 0.21, a Zanazzi-Jona R-factor  $2 \times RRZJ$  of 0.34 and a Pendry R-factor  $2 \times RPE$  of 0.45. All other structural models in the long list that were examined can now be rejected.

Our present results do not change the discussion of Reference 2 about the nature of the Ir(100), Pt(100), Au(100) and Au(111) reconstructions, except for obvious slight modifications in numerical values (see also Ref. 19 for further discussions on this topic).

It appears that the incomplete set of previous data was essentially sufficient to make a structural determination, probably because it included a large number of important peak positions. However, the reliability of the determina-

tion is clearly enhanced by the use of the fast video camera and of R-factors in the present study.

#### ACKNOWLEDGMENTS

This work was supported by the Director, Office of Energy Research, Office of Basic Energy Sciences, Materials Sciences Division of the U.S. Department of Energy under Contract DE-AC03-76SF00098, and by the Deutsche Forschungsgemeinschaft (DFG).

#### REFERENCES

1. M.A. Van Hove, R.J. Koestner, P.C. Stair, J.P. Biberian, L.L. Kesmodel, I. Bartos and G.A. Somorjai, *Surface Sci.* 103, 189 (1981).
2. M.A. Van Hove, R.J. Koestner, P.C. Stair, J.P. Biberian, L.L. Kesmodel, I. Bartos and G.A. Somorjai, *Surface Sci.* 103, 218 (1981).
3. P. Heilmann, E. Lang, K. Heinz and K. Muller, *Appl. Phys.* 9, 247 (1976).
4. E. Lang, P. Heilmann, G. Hanke, K. Heinz and K. Muller, *Appl. Phys.* 19, 287 (1979).
5. P. Heilmann, E. Lang, K. Heinz and K. Muller, *Proceedings of the Conference on Determination of Surface Structure by LEED, Yorktown Heights (1980)*, Plenum Press, in press.
6. K. Heinz and K. Muller, in: *Structural Studies of Surfaces*, Ed. G. Hohler, Springer Tracts in Modern Physics, Vol. 91, Berlin-Heidelberg-New York (1982).
7. K. Strauss, Diploma work, Erlangen (1981).
8. K. Muller, E. Lang, L. Hammer, W. Grimm, P. Heilmann and K. Heinz, *Proceedings of the Conference on Determination of Surface Structure by LEED, Yorktown Heights (1980)*, Plenum Press, in press.
9. J.R. Noonan and H.L. Davis, *J. Vac. Sci. Technol.* 17, 194 (1980).
10. M.A. Stevens and G.J. Russel, *Surface Sci.* 104, 354 (1981).
11. M.A. Van Hove and S.Y. Tong, *Surface Crystallography by LEED*, Springer-Verlag (Heidelberg), 1979.

12. G.O. Arbman and S. Hoernfelt, J. Phys. F2, 1033 (1972).
13. R. Feder, private communication.
14. E. Zanazzi and F. Jona, Surface Sci. 62, 61 (1977).
15. J.B. Pendry, J. Phys. C13, 937 (1980).
16. See, for example: L.L. Kesmodel, L.H. Dubois and G.A. Somorjai, J. Chem. Phys. 70, 2180 (1979).
17. R. Feder, H. Pleyer, P. Bauer and N. Muller, Surface Sci. 109, 419 (1981).
18. D.L. Adams, H.B. Nielsen and M.A. Van Hove, Phys. Rev. B20, 4789 (1979).
19. P. Heilmann, K. Heinz and K. Muller, Surface Sci. 83, 487 (1979).

TABLE I. Best Top Layer Spacings (to Nearest Grid Point) and Corresponding R-Factors For Different Groups of Trial Structures For Ir(100)(1 x 5)

Model Group	Best Spacing (Å)	Five-R-Factor Average	2 x RRZJ	2 x RPE
hexagonal, bridge, full-buckling	2.0	0.21	0.34	0.51
as above, with Feder correction	2.0	0.21	0.34	0.45
hexagonal, bridge 2/3-buckling	2.1	0.27	0.47	0.64
hexagonal, center/top, full-buckling	1.82	0.37	0.55	0.93
hexagonal, center/top, planar	1.82	0.35	0.54	0.86
shifted-rows, 5-cluster	2.02	0.39	0.62	1.00
shifted-rows, 4-cluster	1.82	0.34	0.57	0.76
shifted-rows, 3-cluster	1.72	0.39	0.62	0.91
CDW, vertical	1.62	0.32	0.49	0.91

FIGURE CAPTIONS

- Figure 1: Spatial resolution of the TV computer system. Upper Panel: Part of an Ir(100)(1 x 5) LEED pattern ( $E = 365$  eV) as displayed on the monitor. The white line indicates a (degenerated) electronic window performing a cut through the  $(\bar{2}\bar{1})$ ,  $(\bar{1}\bar{1})$ ,  $(0\bar{1})$  and  $(1\bar{1})$  spots. The upper right part of the pattern is hidden by the sample holder. Middle Panel: Resulting digitized intensity distribution with a sampling distance corresponding to an angle of  $\approx 0.3^\circ$ . Lower Panel: The same at an expanded scale.
- Figure 2: Demonstration of proper and improper background determination for narrowly neighbored spots. See text for explanation.
- Figure 3: Influence of inaccurate incident beam alignment: The  $(1,1/5)$  and  $(\bar{1},1/5)$  beam spectra are compared at an angle of incidence less than  $0.5^\circ$  and less than  $0.2^\circ$  off normal, respectively.
- Figure 4: Symmetrically equivalent (10) beam spectra as an example for the precision of the angle of incidence adjustment and the result of the averaging procedure for cancelling residual deviations.
- Figure 5:  $(1\bar{1})$  beam spectra (averaged), demonstrating that a sweep rate increase by two orders of magnitude shows practically no influence on the I-V profiles.
- Figure 6: Part of the experimental data set. All spectra are averaged (at least four equivalent beams) and normalized with respect to the incident current. ( $T \approx 100$  K;  $\Delta E = 0.5$  eV)
- Figure 7: As Figure 6, for other beams. The  $(1,4/5)$  beam was not measured between 350 and 400 eV because of very weak intensity and simultaneously strong neighbors.

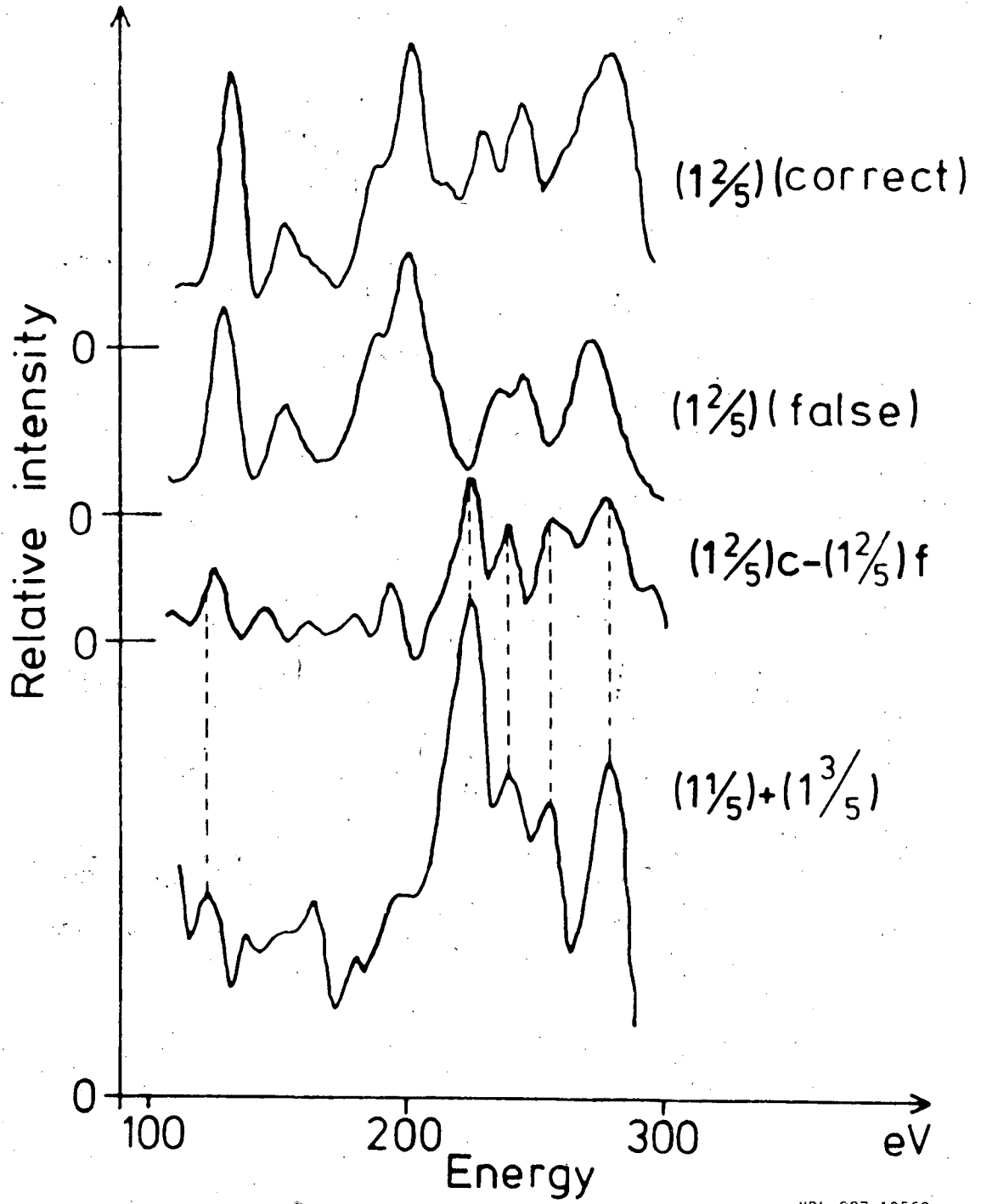


Fig. 2

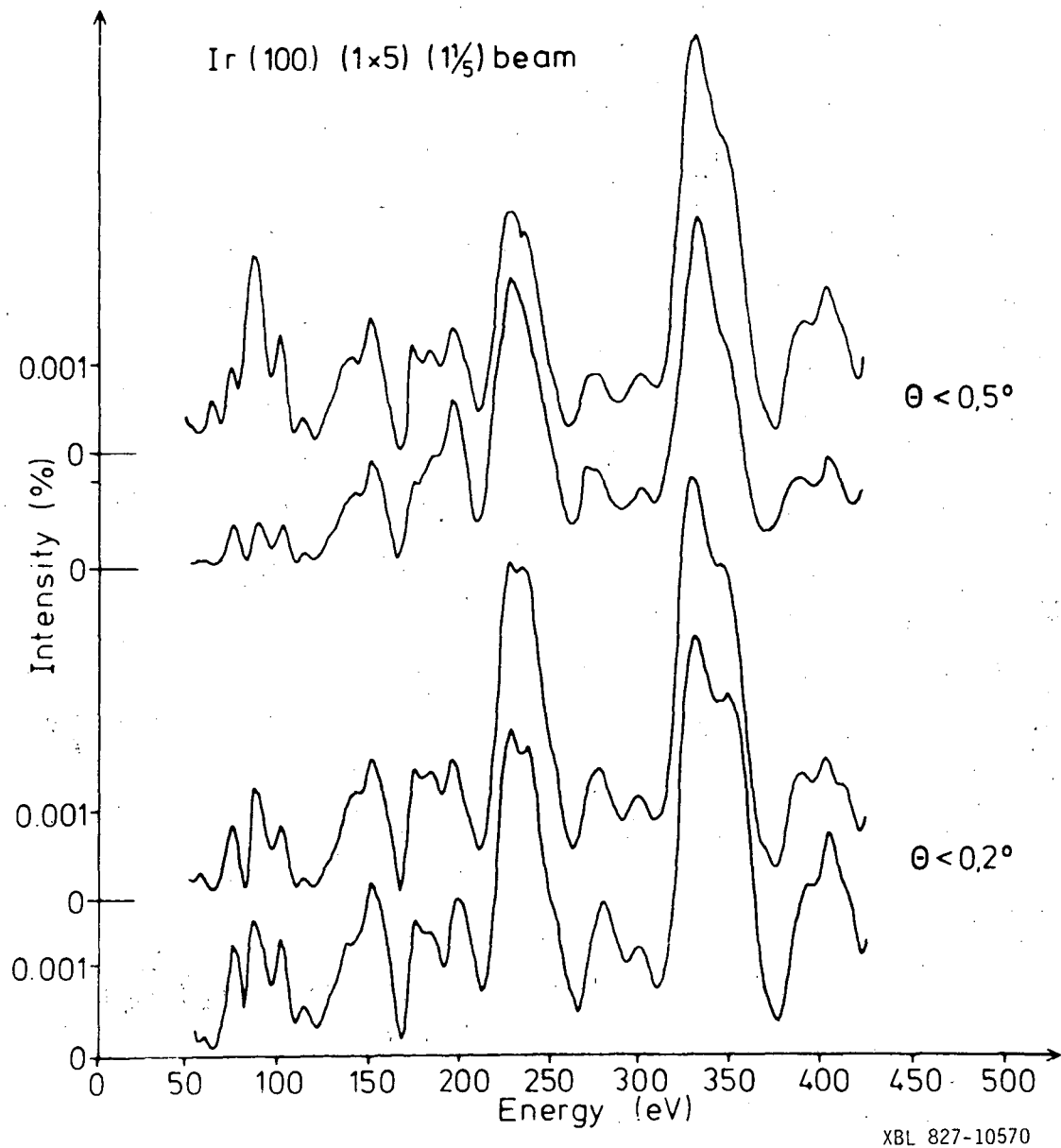


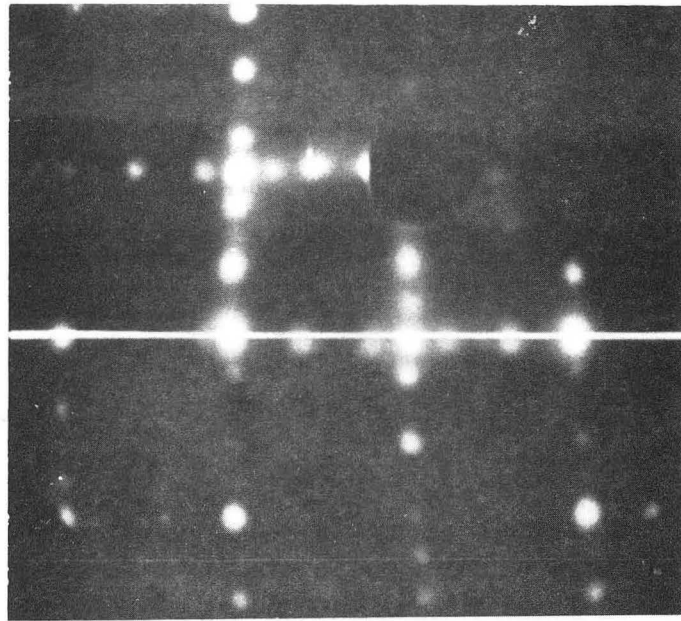
Fig. 3

Figure 8: Comparison of two sets of experimental I-V curves for Ir(100)(1 x 5) taken at normal incidence. The intensity scale for each I-V curve has been adjusted independently. The energy is referred to the Fermi level. The Erlangen data were taken at a temperature of  $\approx 100$  K, the Berkeley data at  $\approx 310$  K. The latter have been shifted by 6 eV to higher energies compared to Reference 2.

Figure 9: Quasi-hexagonal model for Ir(100)(1 x 5) with two registries. Side views, parallel to the surface, are shown at top, exhibiting "full buckling" (see text). Views from top are shown at bottom. Thick circles represent atoms closer to the viewer than thin circles.

Figure 10: Average over five R-factors for some quasi-hexagonal models of Ir(100)(1 x 5). a) Constant full buckling for bridge registry and variable spacing between substrate and reconstructed layer, using the Feder-corrected Arbman-Hoernfelt potential. b) as in c) without Feder's correction to the potential. c) as in b) with 2/3 buckling.  $\Delta V$  is a rigid inner potential shift of the theoretical energy scale, which includes the difference between Fermi level and vacuum level.

Figure 11: Experimental (heavy lines) and theoretical (light lines) I-V curves for four beams diffracted from Ir(100)(1 x 5) at normal incidence. The energy is referred to the Fermi level. At left: quasi-hexagonal full-buckled bridge-registered layer with Feder correction to the potential. At center: same without Feder correction. At right: same with 2/3 buckling and no Feder correction. Four layer spacings are shown as labelled next to the theoretical curves.



| | | | |

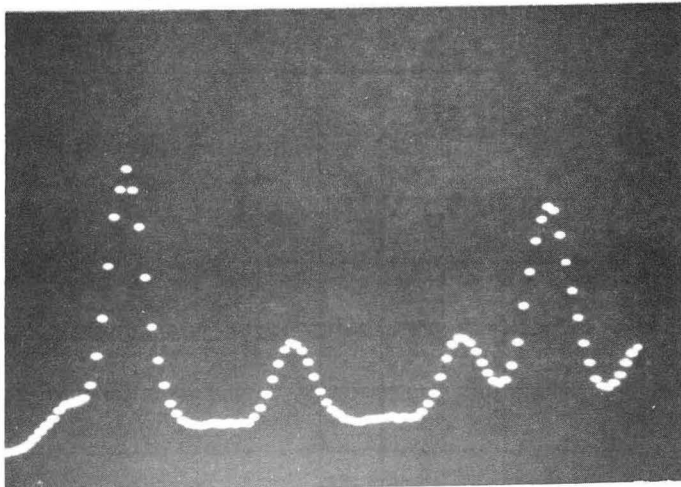
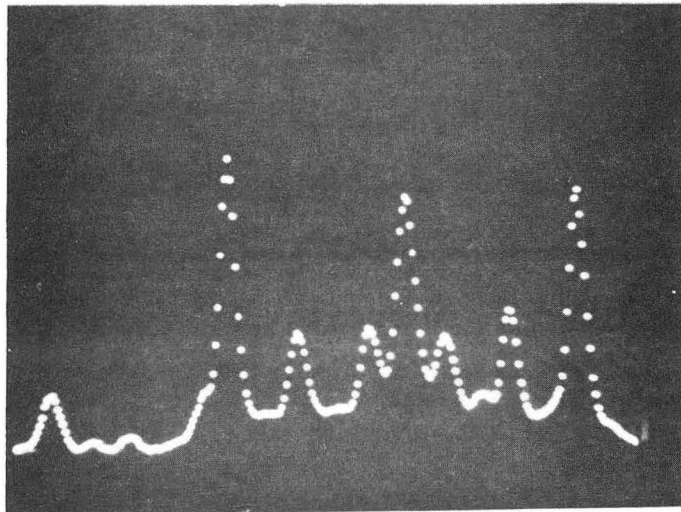


Fig. 1

XBB 827-5857

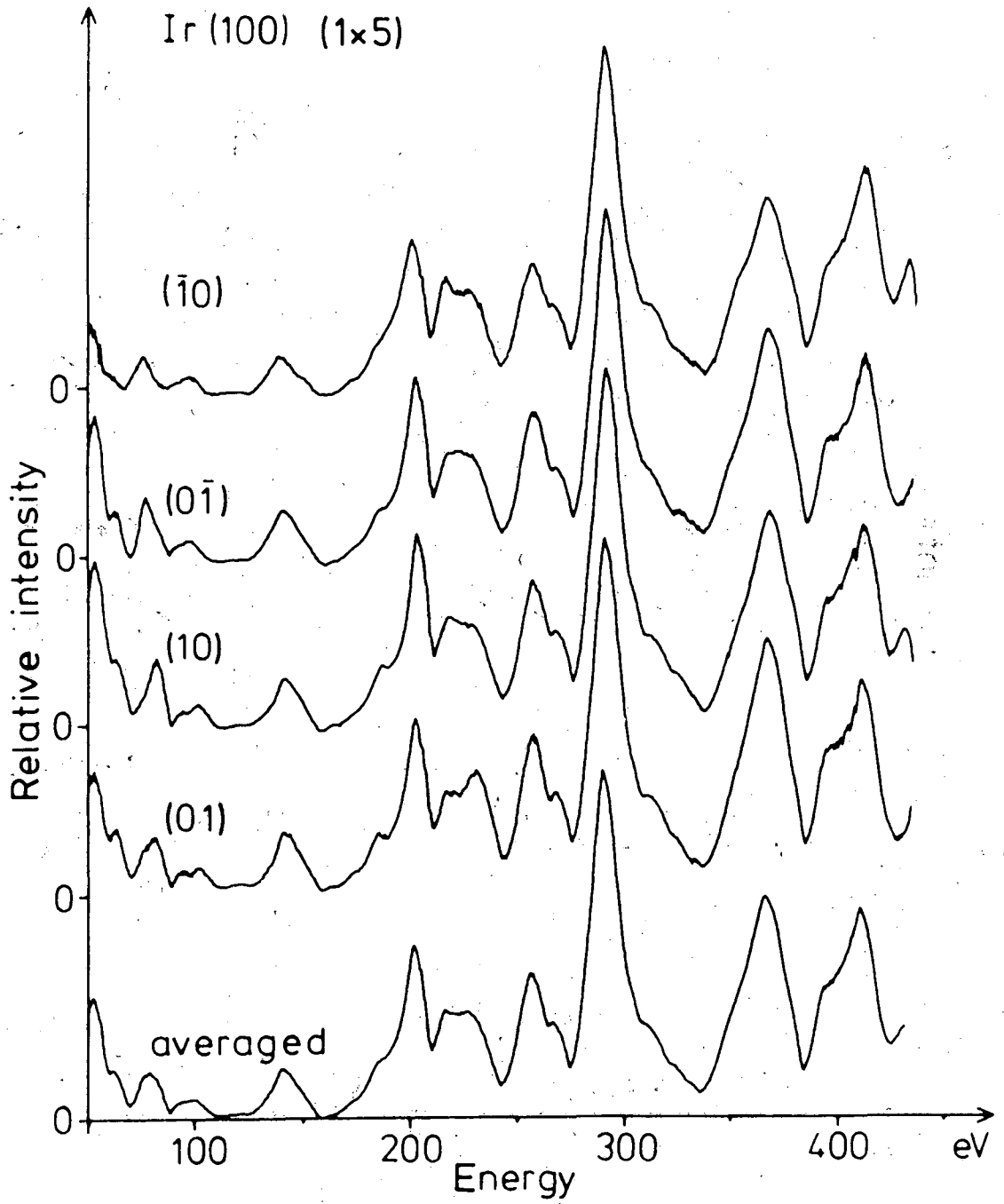


Fig. 4

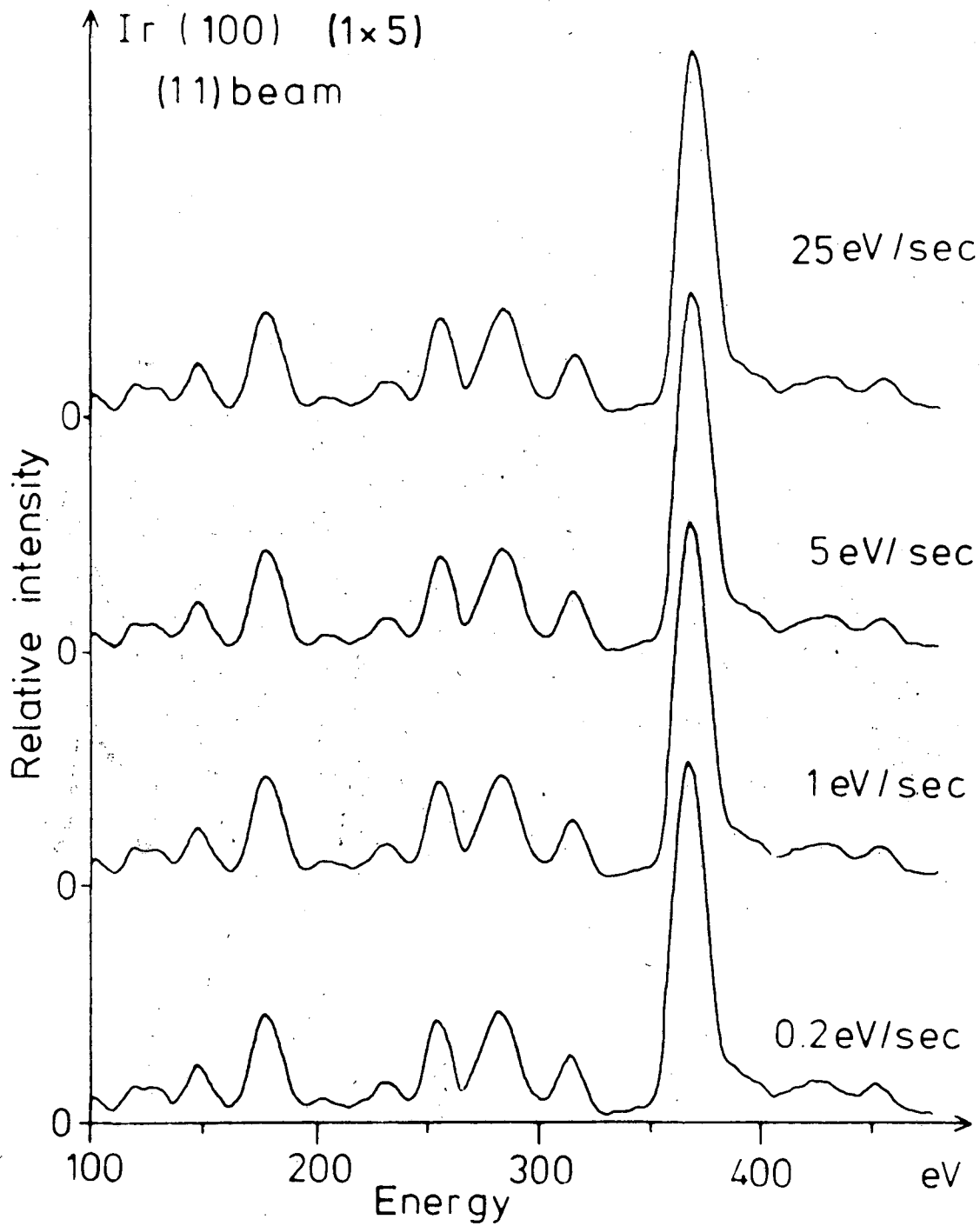
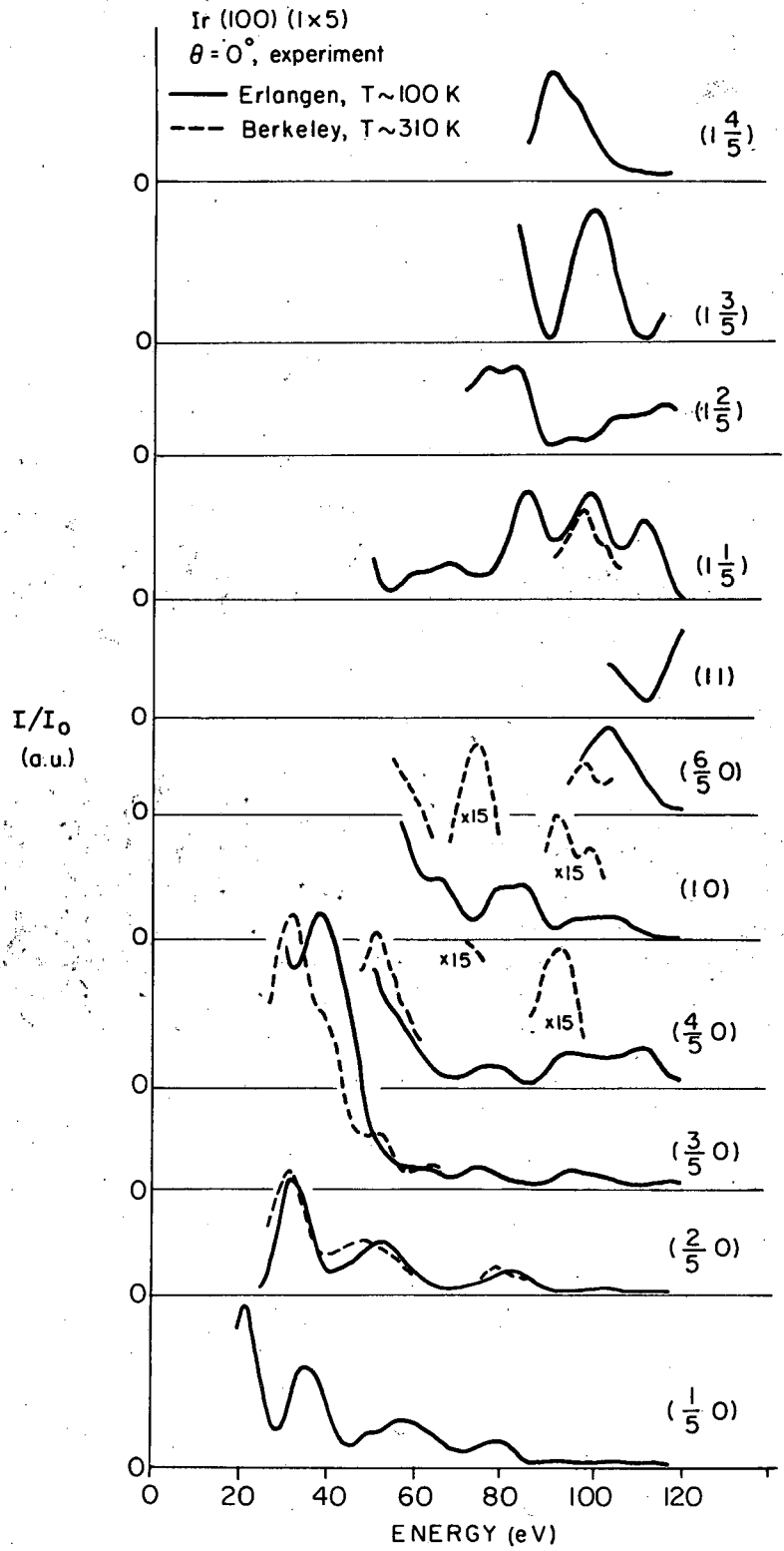


Fig. 5







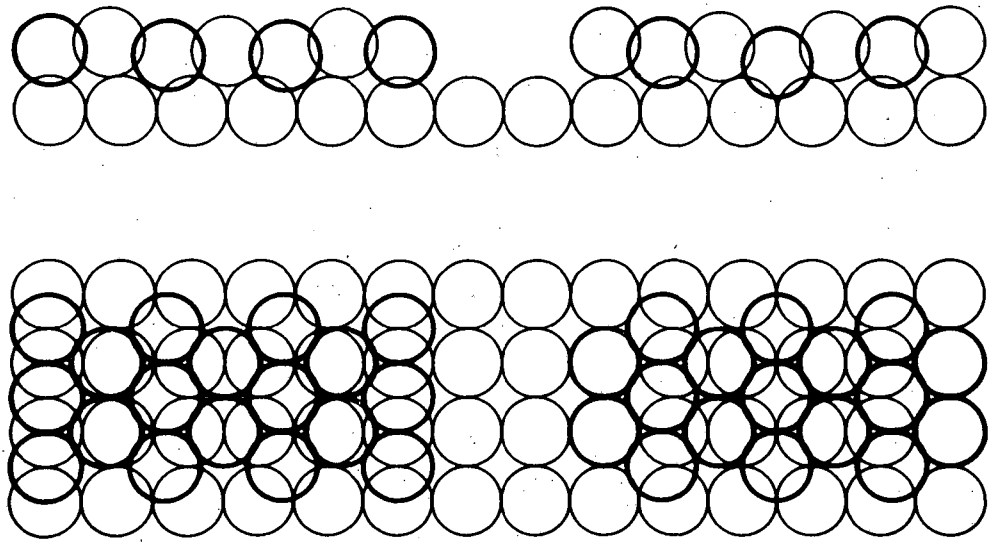
XBL825-5635

Fig. 8

fcc (100) : buckled hexagonal top layer

two-bridge

top/center



XBL 7912-13739

Fig. 9

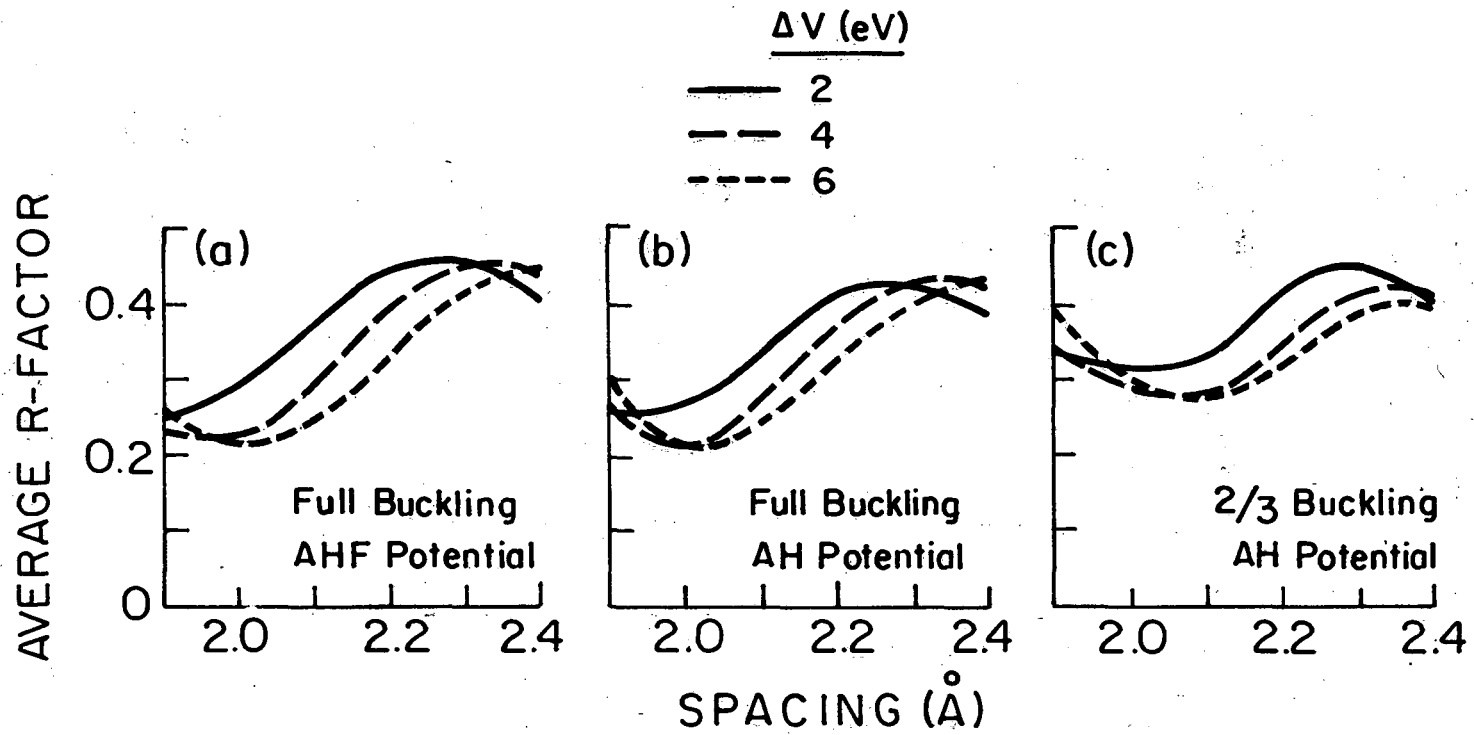


Fig. 10

XBL 825-5634

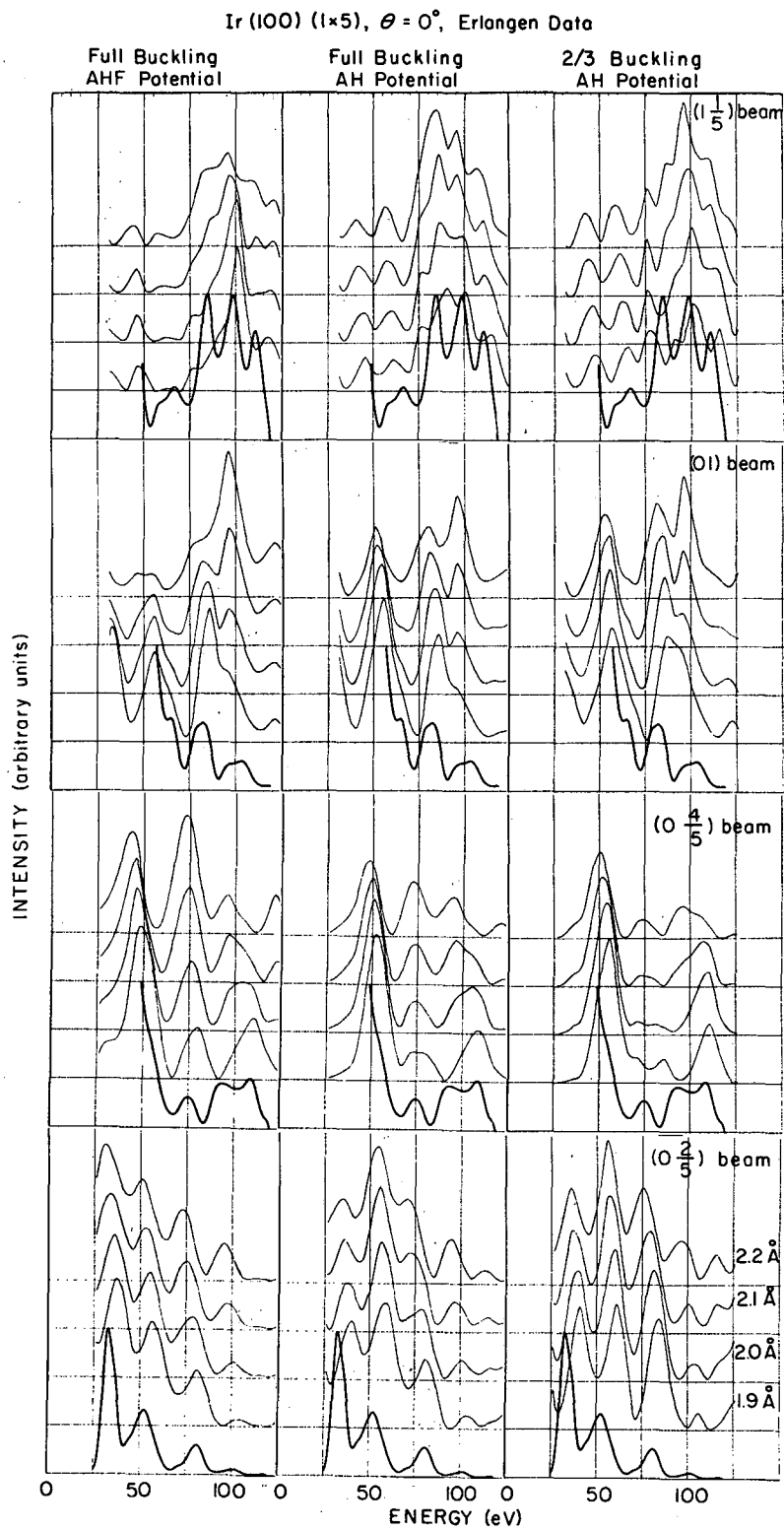


Fig. 11

This report was done with support from the Department of Energy. Any conclusions or opinions expressed in this report represent solely those of the author(s) and not necessarily those of The Regents of the University of California, the Lawrence Berkeley Laboratory or the Department of Energy.

Reference to a company or product name does not imply approval or recommendation of the product by the University of California or the U.S. Department of Energy to the exclusion of others that may be suitable.

TECHNICAL INFORMATION DEPARTMENT  
LAWRENCE BERKELEY LABORATORY  
UNIVERSITY OF CALIFORNIA  
BERKELEY, CALIFORNIA 94720